

RESEARCH ARTICLE

10.1002/2015JB012339

Key Points:

- Seismic waves sampling the inner core beneath Africa show temporal change between 1993 and 2013
- The localized inner core surface temporal change is episodic and alternately enlarged and shrunk
- Inner core surface temporal change rapidly migrates in the time scale of years

Supporting Information:

- Figures S1–S10

Correspondence to:

J. Yao,
kakayao@mail.ustc.edu.cn

Citation:

Yao, J., L. Sun, and L. Wen (2015), Two decades of temporal change of Earth's inner core boundary, *J. Geophys. Res. Solid Earth*, 120, 6263–6283, doi:10.1002/2015JB012339.

Received 7 JUL 2015

Accepted 2 AUG 2015

Accepted article online 6 AUG 2015

Published online 10 SEP 2015

Two decades of temporal change of Earth's inner core boundary

Jiayuan Yao¹, Li Sun^{1,2}, and Lianxing Wen^{1,3}

¹Laboratory of Seismology and Physics of Earth's Interior, School of Earth and Space Sciences, University of Science and Technology of China, Hefei, Anhui, China, ²China Earthquake Networks Center, Beijing, China, ³Department of Geosciences, State University of New York at Stony Brook, Stony Brook, New York, USA

Abstract We report two decades of changing behavior of the Earth's inner core boundary (ICB), which provides the simplest explanation for the observed temporal change of the compressional seismic waves that are reflected from the ICB (PKiKP) and refracted in the inner core (PKIKP), from earthquake doublets occurring in South Sandwich Islands between 1993 and 2013. In the early period (before 2003), the ICB is enlarged beneath the western coast of Gabon, Republic of Congo, and southwest Tanzania in the reflected points of the PKiKP observed at seismic stations OBN, AAK, and ARU, while it experiences little change beneath Zimbabwe or/and Kenya, and beneath west Angola or/and north Central African Republic, in the PKiKP entry or/and exit points of AAK and ARU observations, respectively. In the later period (after 1998), the ICB regions beneath the western coast of Gabon, Republic of Congo, and southwest Tanzania either shrink or remain unchanged, and the temporal change migrates to beneath Zimbabwe or/and Kenya, and beneath west Angola or/and north Central African Republic, with a decrease of inner core surface by 5.59 km between 1998 and 2009 beneath Zimbabwe or Kenya and by 1.73 km beneath west Angola or north Central African Republic between 1998 and 2013. These results indicate that ICB temporal change occurs in localized regions and is episodic, rapidly migrating, and alternately enlarged and shrunk.

1. Introduction

The nature of Earth's inner core boundary (ICB) provides key information about the inner core solidification process [Jacobs, 1953] and, thus, the driving forces for thermo-compositional convection in the outer core [Braginsky, 1963] and the Earth's geodynamo [Davies, 1979; Gubbins, 1977; Loper, 1978]. The traditional views have been that the inner core growing process is geologically slow and geographically uniform, due to the vigorous small-scale convection in the outer core [Buffett, 2000; Fearn *et al.*, 1981; Loper and Roberts, 1981; Stevenson, 1987; Stevenson *et al.*, 1983; Yoshida *et al.*, 1996]. Recent studies, however, revealed that the ICB is locally enlarged by 0.98–1.75 km beneath Africa between 1993 and 2003, and exhibits significant topography [Cao *et al.*, 2007; Dai *et al.*, 2012; Song and Dai, 2008; Wen, 2006]. Nevertheless, the inferred behavior of ICB temporal change was based on a short time frame of the seismic observations and is far from representative. Here we report a survey of two decades of temporal change behavior of the inner core surface, inferred from the temporal changes of the seismic compressional waves that are reflected from the ICB (PKiKP) and refracted in the inner core (PKIKP) (Figure 1a) from nine earthquake doublets occurring in South Sandwich Islands (SSI) between 1993 and 2013.

We study the temporal change of the Earth's inner core surface by analyzing the changes of PKiKP and PKIKP (PKPdf) travel times of earthquake waveform doublets occurring between 1993 and 2013 in SSI (Figures 1a and 2). An earthquake waveform doublet is defined as a pair of earthquakes of similar waveforms occurring at different times but in almost exactly the same location. The change of travel time and waveform of a waveform doublet is sensitive only to the relative change of hypocenters and temporal change of medium properties. Because the relative hypocenter change between the doublets is small and can be accurately accounted for, the doublets have, thus, been used as a powerful data set to detect temporal change of seismic properties inside the Earth [Li and Richards, 2003; Long and Wen, 2012; Poupinet *et al.*, 1984; Poupinet and Souriau, 2001; Poupinet *et al.*, 2000; Song, 2001; Tkalčić *et al.*, 2013; Zhang *et al.*, 2008, 2005]. We present a detailed procedure of searching doublets in section 2 and temporal change of the ICB in section 3, compare two possible explanations of temporal travel time change in section 4, and discuss possible mechanisms and implications of the temporal change in section 5.

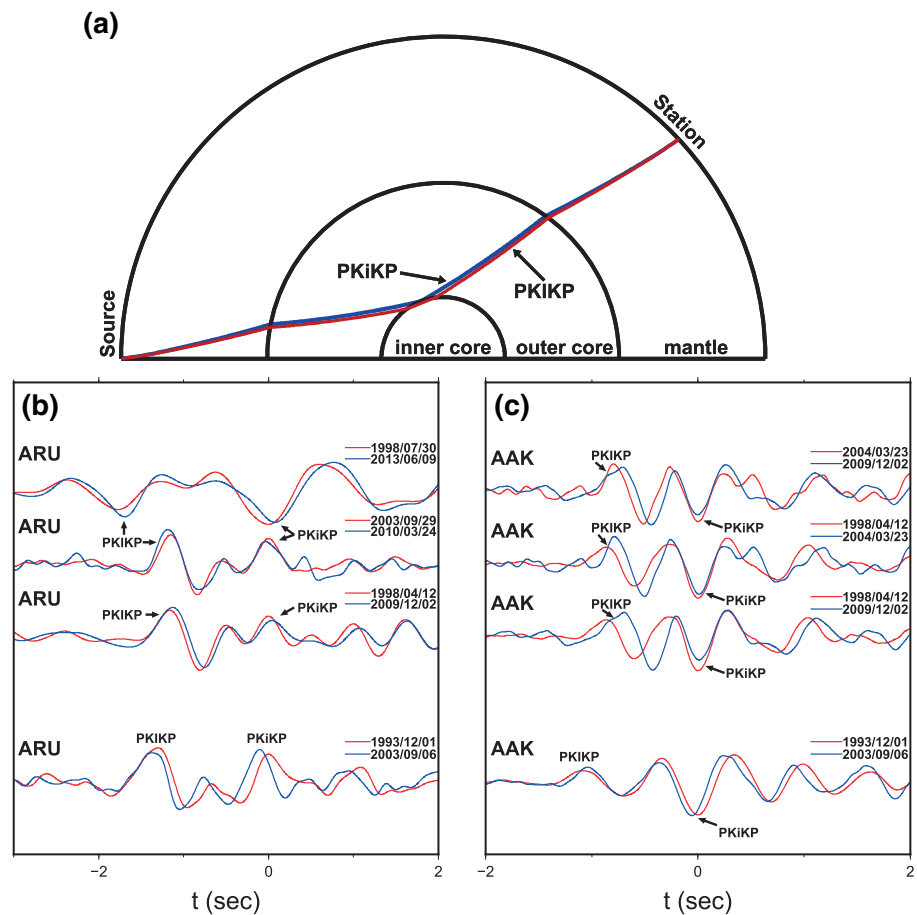


Figure 1. Raypaths of the seismic phases and some examples of waveform comparison between doublets. (a) Raypaths of PKiKP (red) and PKiKP (blue) waves. (b and c) Superimposed PKiKP-PKiKP waveforms recorded at stations (b) ARU and (c) AAK. Waveforms are self-normalized, with those of the earlier occurring events (red traces) aligned along with the handpicked PKiKP phases and those of the later events (blue traces) superimposed with time shifts that account for the differences in the best fitting relative location and origin time of the doublets. Waveforms at ARU for doublet 9804/0912 are filtered from 0.8 to 2.0 Hz. Other waveforms are filtered with the WWSSN-SP instrument response, and the waveforms at ARU for doublet 9807/1306 are further filtered from 0.5 to 1.0 Hz.

2. Doublets in South Sandwich Islands

We search doublets in two steps from all the earthquakes occurring between 1993 and 2013 in SSI (55°S–62°S and 30°W–23°W), with body wave magnitude m_b above 4.7 in the PDE (Preliminary Determination of Epicenters) catalog. The database is consisted of 1420 events. Seismic data are collected from the Global Seismographic Network, the Canadian National Seismographic Network, the Kyrgyz Seismic Telemetry Network, the United States National Seismic Network, the Caltech Regional Seismic Network, and some other regional networks.

The first step of doublet screening is based on the initial earthquake catalog locations and waveform cross-correlation coefficients between the events. Events separated by less than 60 km are considered as potential doublets. The vertical seismic waveforms are used for doublet search and are filtered in the frequency range of 0.8–2.0 Hz. We calculate the cross-correlation coefficients between waveforms of all potential doublets, in a 30 s time window starting 15 s before the predicted P arrival. Event pairs that have cross-correlation coefficients larger than 0.95 are selected for further manual relocation. The first step of the screening yields 32 potential event pairs.

In the second step, a master event algorithm [Wen, 2006] is applied to determine the relative location and origin time between 32 event pairs yielded in the first step of screening. The algorithm treats one event of

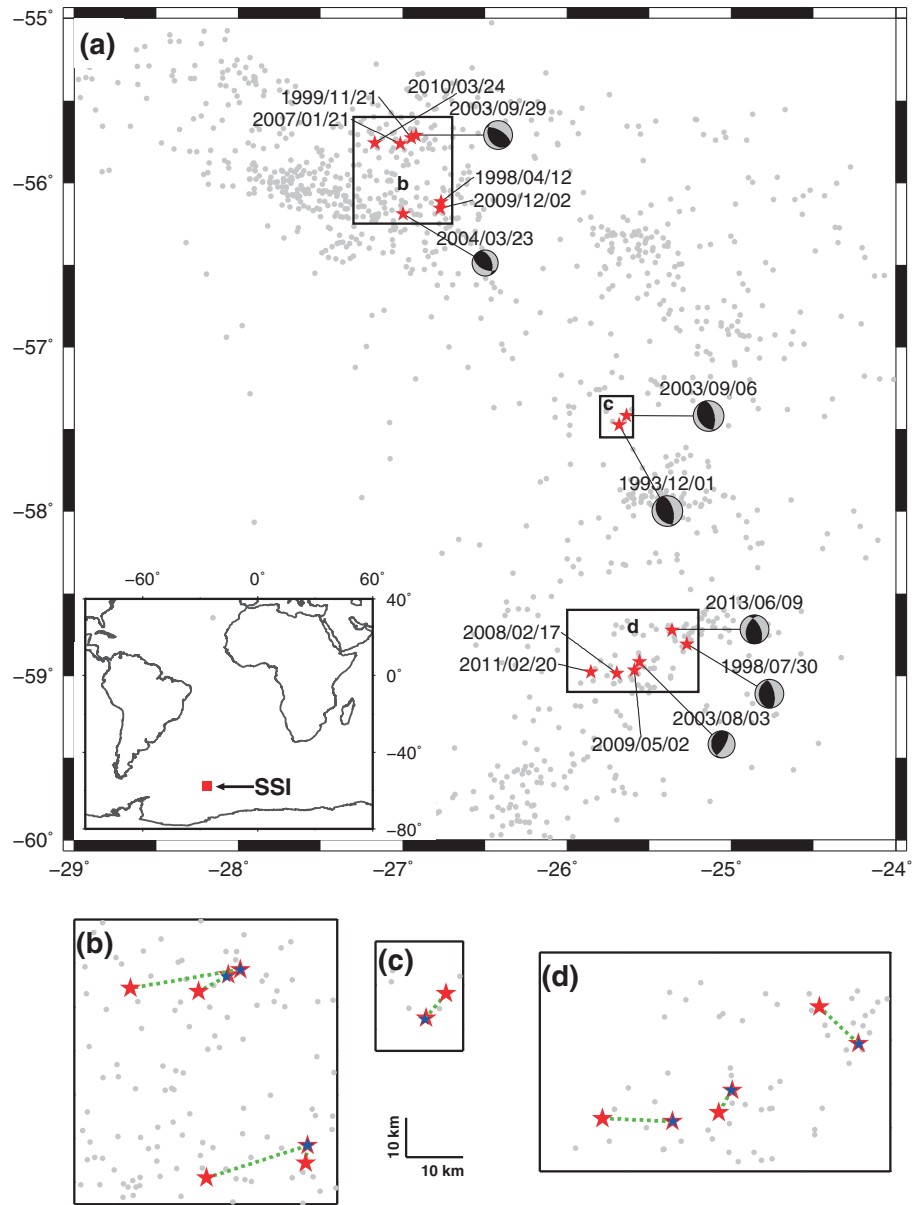


Figure 2. (a) Regional map of earthquake doublets (red stars) and seismicity (gray dots) near the South Sandwich Islands (SSI). Doublets are labeled with event date and their available Global Centroid Moment Tensor (CMT) [Dziewonski *et al.*, 1981; Ekström *et al.*, 2012]. The geographical location of SSI is shown in the lower-left inset. Boxes b–d indicate positions for Figures 2b–2d below. (b–d) Best fitting relative positions (blue stars) of the later events relative to the master events, with green dashed lines connected with their catalog positions. Source parameters of the doublets are listed in Table 1.

the pair as the master event (in the present case, the earlier event) and fixes its origin time and hypocenter location to be that of the PDE catalog. For an assumed location and depth, the travel time residuals in the individual stations are calculated by subtracting the predicted relative arrival times of the seismic phases from the measured arrival time differences between the event pair [Wen, 2006]. The best fitting relative origin time and hypocenter location of the second event (in present case, the later event) are determined by minimizing the root-mean-square (RMS) travel time residual of the seismic phases between the event pair through grid searching.

The non-IC phases (seismic phases that are not associated with the inner core) are used in the relocation, including the direct compressional wave in the mantle (P), the surface reflected compressional wave in the

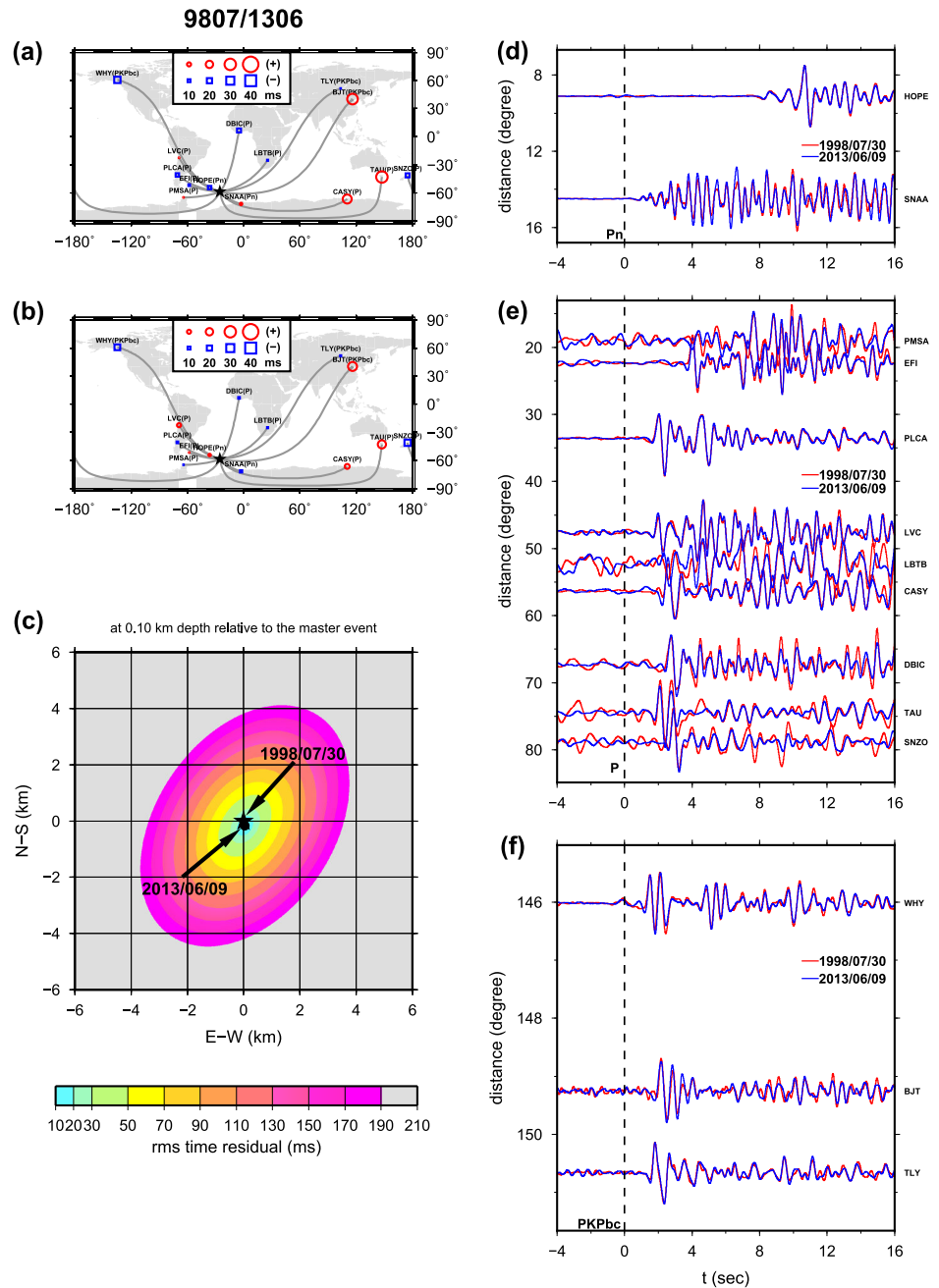


Figure 3. Relocation results and waveforms for doublet 9807/1306. (a) Measured differences in absolute arrival times (circles and squares) of non-IC phases between the doublet plotted at the location of each station, along with the great circle paths (gray lines) from the doublet (star) to the stations. The arrival time differences are plotted with respect to an origin time that generates a zero mean of the arrival time differences for all the stations. The circles indicate that the non-IC phases in the later event arrive relatively earlier than their counterparts in the earlier event, while the squares show the opposite. Seismic stations and phases are labeled in the figure. (b) Travel time residuals between the doublet calculated by subtracting the predicted relative arrival times of the seismic phases based on the best fitting relative location and origin time of the doublet from the measured arrival time differences, plotted at the location of each station. (c) Best fitting location of the later event (dot labeled as 2013/06/09) relative to the location of the earlier (master) event (0,0) (star labeled as 1998/07/30) that minimizes the RMS travel time residuals of the non-IC phases between the doublet, along with the RMS travel time residuals as a function of relative location of the later event. (d–f) Examples of self-normalized waveforms filtered with the WWSSN-SP instrument response for events 1998/07/30 (red traces) and 2013/06/09 (blue traces) with station names shown in the right side of the panels. Waveforms for the earlier event are aligned by the predicted (d) Pn, (e) P, or (f) PKPbc arrivals predicted based on IASP91 model [Kennett and Engdahl, 1991], whereas waveforms for the later event are aligned according to the travel times predicted based on the best fitting relative location and origin time of the doublet.

Table 1. Doublets in the South Sandwich Islands From 1993 to 2013^a

Doublet ID	Date	Time	Latitude (°N)	Longitude (°E)	Depth (km)	Mag (m_b)	dt (year)	RMS (ms)	t_{err} (ms)	dh_c (km)	dz_c (km)	dh_r (km)	dz_r (km)
	year/month/day	hh:mm:ss.ss											
9312/0309	1993/12/01	00:59:01.50	-57.475	-25.685	33.0	5.5	-	-	-	-	-	-	-
	2003/09/06	15:46:59.90	-57.419	-25.639	33.0	5.6	9.8	16	31	6.81	0.00	0.37	0.70
9807/1306	1998/07/30	23:36:30.64	-58.808	-25.273	33.0	5.1	-	-	-	-	-	-	-
	2013/06/09	00:21:34.64	-58.724	-25.362	33.0	5.3	14.8	13	24	10.66	0.00	0.16	0.10
9804/0912	1998/04/12	21:33:47.42	-56.116	-26.768	100.0	4.7	-	-	-	-	-	-	-
	2009/12/02	23:14:00.83	-56.156	-26.772	59.7	5.4	11.6	17	33	4.45	-40.30	0.04	0.13
9804/0403	1998/04/12	21:33:47.42	-56.116	-26.768	100.0	4.7	-	-	-	-	-	-	-
	2004/03/23	06:20:00.03	-56.190	-26.998	77.5	4.9	5.9	11	21	16.45	-22.50	0.11	-0.10
9911/0701	1999/11/21	10:39:53.08	-55.726	-26.949	33.0	4.8	-	-	-	-	-	-	-
	2007/01/21	15:03:16.37	-55.764	-27.016	47.7	5.6	7.2	9	18	5.95	14.70	0.57	0.68
0308/0905	2003/08/03	05:38:57.55	-58.915	-25.561	33.0	4.9	-	-	-	-	-	-	-
	2009/05/02	22:27:07.92	-58.966	-25.591	48.6	4.7	5.8	8	23	5.93	15.60	0.11	0.11
0309/1003	2003/09/29	22:07:05.46	-55.714	-26.921	33.0	4.9	-	-	-	-	-	-	-
	2010/03/24	03:06:19.67	-55.757	-27.172	35.9	4.9	6.5	7	14	16.43	2.90	0.01	0.01
0403/0912	2004/03/23	06:20:00.03	-56.190	-26.998	77.5	4.9	-	-	-	-	-	-	-
	2009/12/02	23:14:00.83	-56.156	-26.772	59.7	5.4	5.7	13	37	14.49	-17.80	0.15	-0.20
0802/1102	2008/02/17	19:32:09.10	-58.986	-25.697	66.5	4.9	-	-	-	-	-	-	-
	2011/02/20	17:37:37.32	-58.979	-25.857	10.0	5.0	3.0	9	21	9.20	-56.50	0.04	0.00

^adt: time separation between the doublet. RMS: root-mean-square time residual between the doublet for the best fitting relative location and origin time. t_{err} : the maximal travel time residual in the individual stations between the doublet for the best fitting relative location and origin time. dh_c and dz_c : horizontal and vertical separation between the doublet in the PDE catalog, respectively. dh_r and dz_r : horizontal and vertical separation between the doublet after the relocation, respectively. Other parameters of the events of each doublet are from the PDE catalog.

mantle (pP), and the two branches of the compressional waves traveling in the outer core (PKPbc and PKPab) (Figures 3a, 3b, and 3d–3f). The waveforms are simply filtered with the worldwide standard seismic network short-period (WWSSN-SP) instrument response. The travel time differences of all the phases between the doublets are obtained by cross-correlating the waveforms between the doublets. To achieve subsample rate precision, the time series are interpolated to a 0.0025 s sampling rate based on the Wiggins interpolation method [Wiggins, 1976] before the cross correlations are performed. The error of such time picking is ± 0.01 s.

The search region for the relative hypocenter location of the subsequent event is a 10 km (north-south) \times 10 km (east-west) \times 2 km (vertical) box centered at the fixed location and depth of the earlier (master) event (Figure 3c). The search grid intervals are 0.01 km in north-south and east-west directions and 0.001 km in depth. The maximal travel time residual in the individual stations for the best fitting relative location and origin time is considered as the relocation error bar of the event pair.

We are able to find eight high-quality event pairs between 1993 and 2013, which have good data coverage of the non-IC phases to be accurately relocated and are within 1 km of separation of depth and horizontal distance between them (Figure 2 and Table 1). These eight event pairs are considered as doublets and are used to study the temporal change of the inner core surface, in combination with doublet 9312/0309 used by some authors earlier [e.g., Wen, 2006; Zhang *et al.*, 2005]. The time separation of the doublets ranges from 3.0 to 14.8 years. The RMS travel time residuals of the non-IC phases are smaller than 0.02 s for all the relocations of the doublets, and the relocation error bars range from 0.014 to 0.037 s (Table 1).

3. Temporal Change of the Earth's Inner Core Surface

3.1. Temporal Changes of the PKiKP and PKIKP Waves

The PKiKP-PKIKP waveforms of the doublets are superimposed on the basis of the relative arrival times of these phases between the doublets predicted based on the best fitting relative location and origin time of the doublets (Figures 1b, 1c, 6, 7, and S9 of the supporting information). The PKiKP and PKIKP travel time residuals between the doublets are further calculated by subtracting the predicted relative arrival times of the seismic phases from the measured arrival time differences between the doublets (Figures 5 and S8). If

Table 2. PKiKP and PKIKP Travel Time Residuals and Their Temporal Changes^a

Station	Doublet ID	dt_{err} (s)	PKiKP			PKIKP			$\Delta T_{PKiKP}^{res} - \Delta T_{PKIKP}^{res}$ (s)
			ΔT_{PKiKP}^{res} (s)	$\Delta T_{PKiKP}^{change}$ (s)	ΔR_{ICB} (km)	ΔT_{PKIKP}^{res} (s)	$\Delta T_{PKIKP}^{change}$ (s)	ΔR_{ICB} (km)	
KEV	9807/1306	0.034	0.029	N	N	0.001	N	N	0.028
LVZ	9312/0309	0.041	-0.025	N	N	-0.008	N	N	-0.017
DAG	0308/0905	0.033	-0.042	-0.009	-0.27	0.008	N	N	-0.050
ALE	0802/1102	0.031	0.002	N	N	0.020	N	N	-0.018
	9911/0701	0.028	-0.015	N	N	-0.021	N	N	0.006
	9312/0309	0.041	0.023	N	N	0.040	N	N	-0.017
KIEV	0308/0905	0.033	-0.003	N	N	-	-	-	-
OBN	9807/1306	0.034	0.021	N	N	-	-	-	-
	9312/0309	0.041	0.070	0.029	0.53	-	-	-	-
ARU	9807/1306	0.034	-0.078	-0.044	-1.16	-0.070	-0.036	-1.73	-0.008
	0309/1003	0.024	0.019	N	N	0.024	N	N	-0.005
	9804/0912	0.043	-0.041	N	N	-0.029	N	N	-0.012
	9312/0309	0.041	0.111	0.070	1.78	0.041	N	N	0.070
AAK	9807/1306	0.034	0.007	N	N	-	-	-	-
	0403/0912	0.047	0.002	N	N	-0.078	-0.031	-1.29	0.080
	9804/0403	0.031	-0.005	N	N	-0.085	-0.054	-2.28	0.080
	9804/0912	0.043	-0.011	N	N	-0.171	-0.128	-5.59	0.160
	9312/0309	0.041	0.067	0.026	0.59	-0.041	N	N	0.108
XAN	9807/1306	0.034	-0.007	N	N	0.014	N	N	-0.021
	9312/0309	0.041	-0.025	N	N	-0.002	N	N	-0.023
CHTO	9807/1306	0.034	-0.008	N	N	-	-	-	-
	9312/0309	0.041	0.000	N	N	-	-	-	-
LSA	9807/1306	0.034	-0.032	N	N	0.017	N	N	-0.049
NIL	9807/1306	0.034	0.000	N	N	-	-	-	-

^a dt_{err} : travel time residual error, i.e., the relocation error (Table 1) plus time picking error (0.01 s). ΔT_{PKiKP}^{res} and ΔT_{PKIKP}^{res} : travel time residuals of PKiKP and PKIKP phases between the doublets, respectively. Positive indicates that the seismic phases arrive earlier in the later event, while negative indicates the opposite. $\Delta T_{PKiKP}^{change}$ and $\Delta T_{PKIKP}^{change}$: temporal change of PKiKP and PKIKP travel times between the doublets, respectively (travel time residuals beyond travel time residual error of each doublet, dt_{err}). $\Delta T_{PKiKP}^{res} - \Delta T_{PKIKP}^{res}$: PKiKP-PKIKP differential travel time residuals. ΔR_{ICB} : temporal change of the radius of the inner core surface corresponding to the temporal change in PKiKP or PKIKP travel times ($\Delta T_{PKiKP}^{change}$ or $\Delta T_{PKIKP}^{change}$) between the doublets. Readers should keep in mind that *Wen* [2006] took PKiKP arrival times as reference to calculate the temporal change in PKiKP travel times at ARU and AAK for doublet 9312/0309 and assumed PKIKP travel time residual at AAK for this doublet is zero, while our reported values of travel time changes are based on absolute travel time residuals beyond possible travel time residual error. "N" means no change beyond the detection limit (i.e., travel time residual for PKiKP or PKIKP is zero or within possible total residual error) (Table 3).

the superimposed waveforms are noticeably in misalignment between the doublets, or if the magnitudes of travel time residuals are larger than travel time residual error, i.e., the relocation error (Table 1) plus time picking error (0.01 s), it would mean that the arrival times of the seismic phases between the doublets cannot be explained by the origin time and hypocenter difference of the doublets, and they exhibit temporal change (Table 2).

3.1.1. Temporal Changes of the PKiKP Waves Sampling Africa

The temporal changes of the PKiKP waves are observed in the doublet data recorded in three seismic stations, OBN (Obninsk, Russia), ARU (Arti, Russia), and AAK (Ala Archa, Kyrgyzstan). These temporal changes are geographically confined in the east by the PKiKP waves from the SSI doublets to stations ALE, DAG, LVZ, and KEV (region a, Figure 4a) and the west by the PKiKP waves from the doublets to stations NIL, LSA, CHTO, and XAN (region e, Figure 4a), both of which paths do not exhibit discernible temporal PKiKP travel time change between all the doublets (Figures 5a and 5e, and Table 2). *Wen* [2006] reported that PKiKP phases recorded at OBN, AAK, and ARU arrive at least 0.039 to 0.07 s [travel time residual (for OBN) beyond the relocation error of 0.031 s of the doublet or PKiKP-PKIKP differential travel time residuals (for ARU and AAK)] earlier in the 2003 event as compared to the 1993 event in doublet 9312/0309. Taking into account both the relocation and time picking errors (with the total of 0.041 s), PKiKP phases for these stations arrive at least 0.026 to 0.07 s (absolute travel time residuals beyond the total error) earlier in the 2003 event (Figures 1b, 1c, and 5b–5d, and Table 2). However, no discernible travel time differences of the PKiKP phases are observed at OBN and AAK between the doublets in the later periods (doublets 9804/0912, 9804/0403, 0403/0912, and 9807/1306) (Figures 1c, 5b, 5d, 6b, and 6d, and Table 2). No discernible PKiKP travel time difference is observed at station KIEV (a station nearby OBN; Figure 4a) for doublet 0308/0905

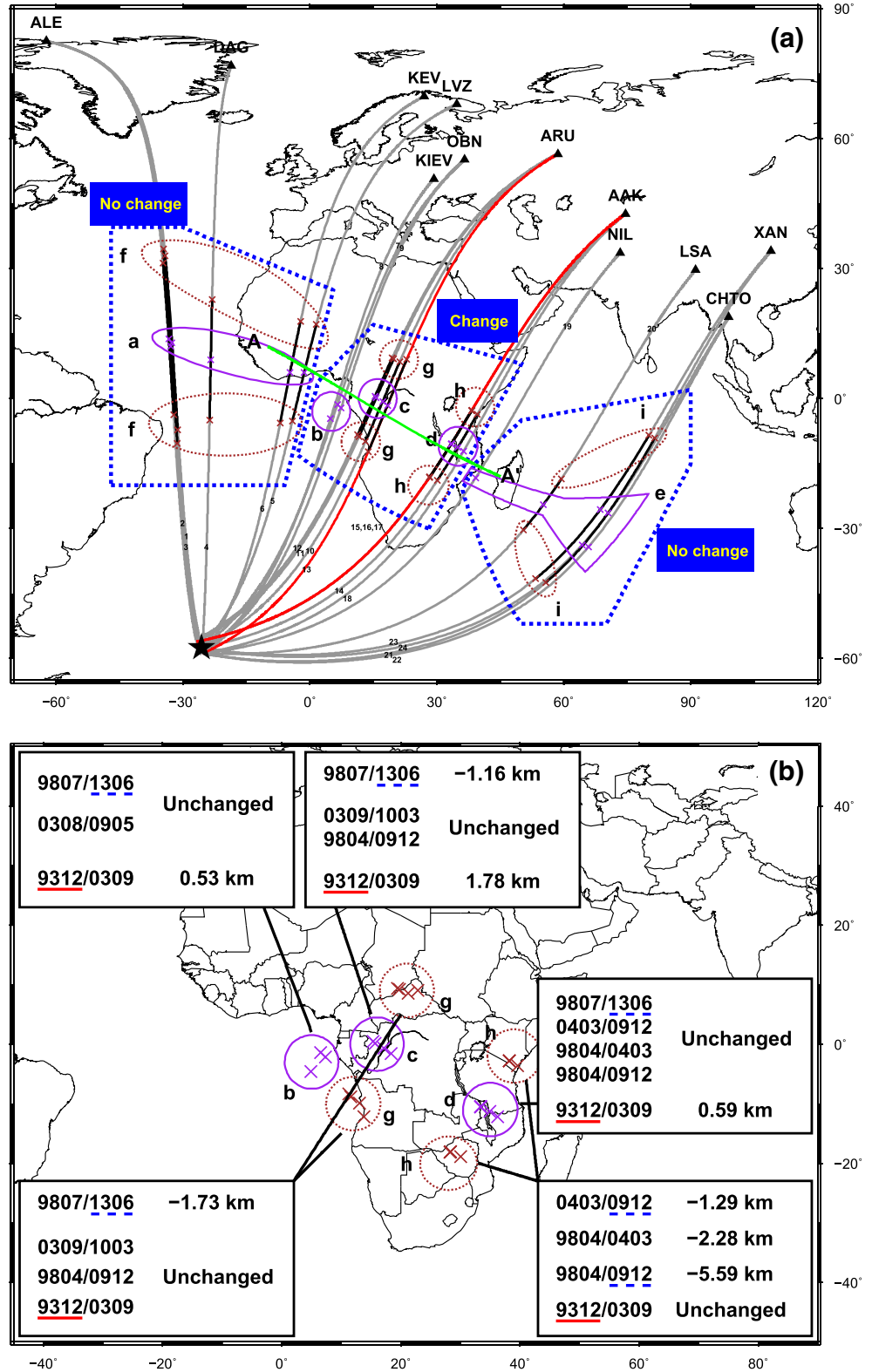


Figure 4

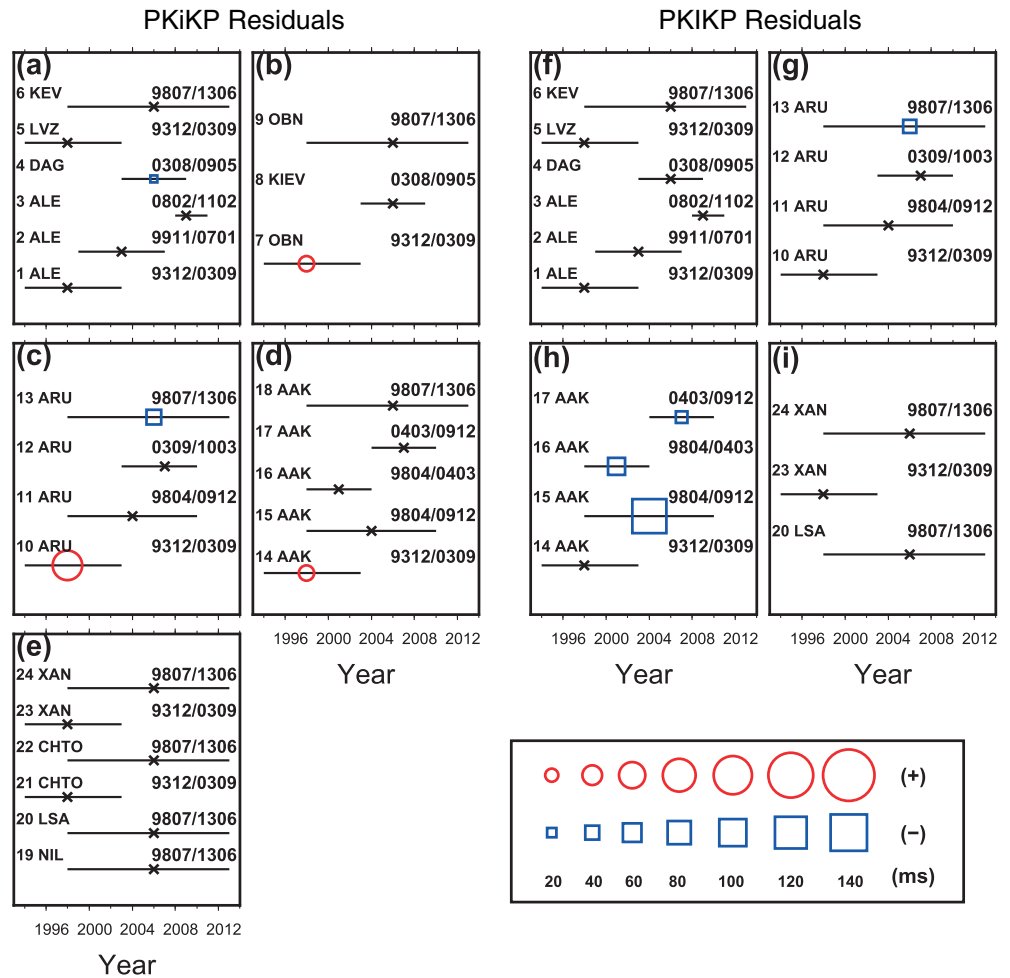


Figure 5. Temporal changes (symbols) of (a–e) PKiKP and (f–i) PKIKP travel times between the doublets, i.e., travel time residuals between the doublets beyond the possible travel time residual error of each doublet. Travel time residuals are calculated by subtracting the predicted relative arrival times of the seismic phases based on the best fitting relative origin time and hypocenter position of the doublets from the measured arrival time differences between the doublets (Table 2). The possible travel time residual error is the summation of time picking error and the relocation error for the doublet. Red circles indicate that the seismic phases arrive earlier in the later event, while blue squares indicate the opposite. The black crosses mean that the magnitudes of travel time residuals are smaller than the possible travel time residual errors of the respective doublets. Each travel time residual is plotted centered in the time span of the doublet (black bar) and is labeled with a number and station name on the left, with the associated seismic waveforms between the doublet shown in Figure 6 and labeled in the same way.

Figure 4. (a) Great circle paths (gray lines, labeled in accordance with the seismograms in Figure 6 with the same numbers) from doublets (star) to stations (triangles), PKiKP reflection points at the ICB (purple crosses), PKiKP entry and exit points at the ICB (brown crosses) and PKiKP raypaths in the inner core (black lines). Two red lines (ARU and AAK) and one green line (AA) indicate the cross sections where temporal change of ICB is illustrated in Figures 12a–12c. Circles and polygons (purple for PKiKP and brown for PKIKP) indicate approximate groups of similar PKiKP reflection or PKiKP entry/exit points at the ICB (crosses), with corresponding seismic observations presented in the panels in Figure 5 with the same labeling letters. Heavy blue polygons indicate approximate regions that show temporal change (middle, labeled with change) or no temporal change (left and right, labeled with no change). (b) Temporal change of the inner core surface beneath Africa (in the region of the middle heavy blue polygon in Figure 4a). Each small panel lists the doublets and the temporal changes of the inner core surface between the occurrences of doublets for a region, with the region connected by a black line with the panel. Positive and negative values mean the increase and decrease of inner core radius, respectively. “Unchanged” means no change beyond the detection uncertainty (i.e., travel time residual for PKiKP or PKIKP is zero or within possible total residual error) (Tables 2 and 3). Events underlined with red solid and blue dashed lines indicate the earliest and latest occurring event in each panel, respectively.

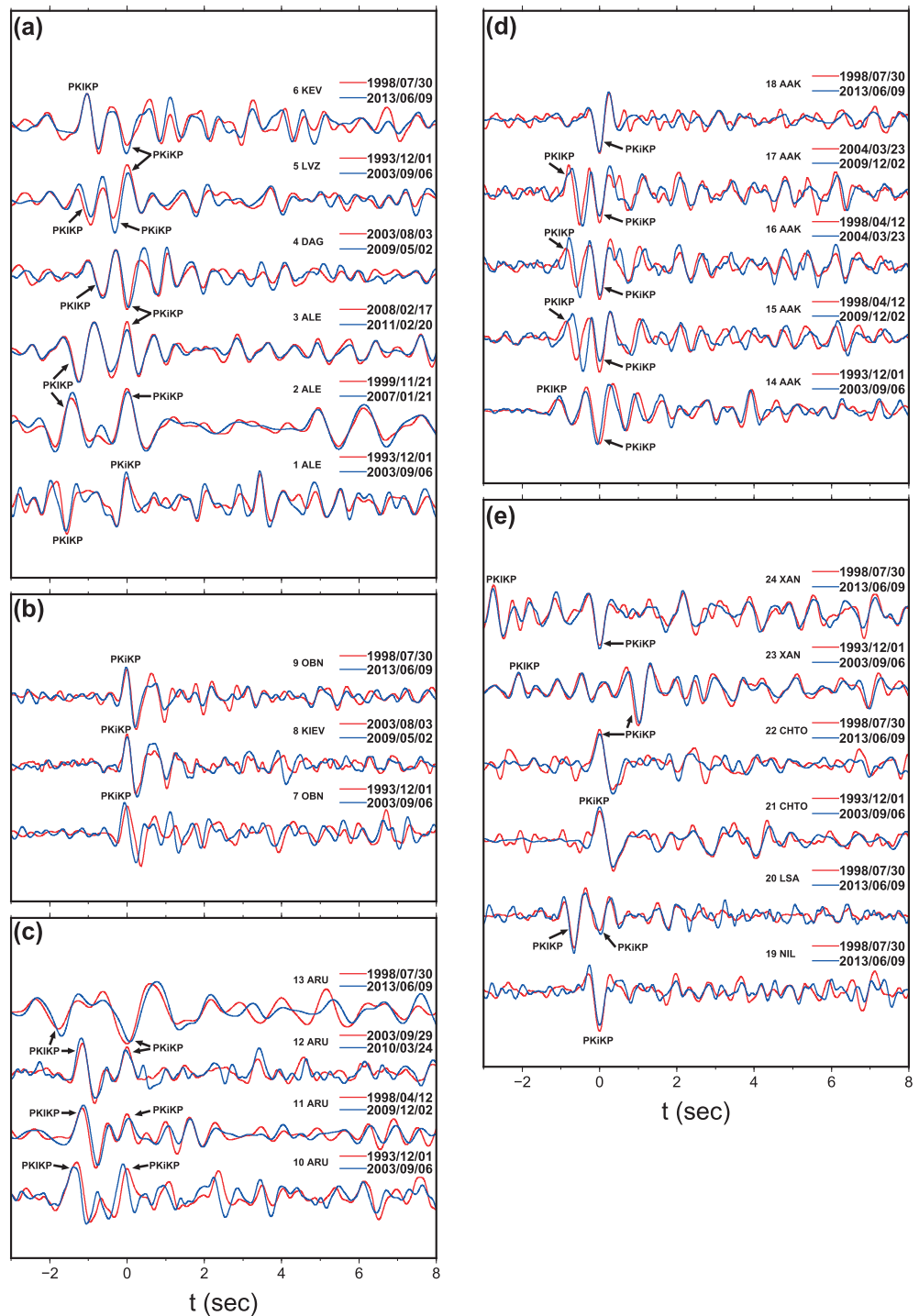


Figure 6. Superimposed PKiKP-PKiKP waveforms of the doublets. The waveforms are processed and aligned in the same way as in Figures 1b and 1c (except that the waveforms at XAN for doublet 9312/0309 are shifted 1 s to the right for display purpose), and are labeled with a number and station name that correspond to those in Figures 4 and 5. Waveforms at ARU for doublet 9804/0912 are filtered from 0.8 to 2.0 Hz. Other waveforms are filtered with the WWSSN-SP instrument response, and the waveforms at ALE for doublet 9911/0701 and ARU for doublet 9807/1306 are further filtered from 0.5 to 1.0 Hz.

either (Figures 5b and 6b, and Table 2). PKiKP temporal travel time change at ARU reverses trend in the doublets in the later periods (Figures 1b, 5c, and 6c, and Table 2). PKiKP arrives later (at least 0.044 s) in the later event for doublet 9807/1306 and exhibits no discernible temporal change between doublets 9804/0912 and 0309/1003.

3.1.2. Temporal Changes of the PKiKP Waves Sampling Africa

PKiKP temporal changes are observed in the seismic data recorded at AAK and ARU. Similar to the PKiKP temporal changes, PKiKP temporal changes are also geographically confined in the east by the PKiKP waves from the SSI doublets to ALE, DAG, LVZ, and KEV (region f, Figure 4a) and the west by the PKiKP waves from the doublets to LSA and XAN (region i, Figure 4a), both of which paths do not show any discernible PKiKP temporal travel time change between all the doublets (Figures 5f and 5i, and Table 2). Most notable PKiKP temporal travel time changes are observed at AAK observations. No discernible PKiKP travel time difference is observed at AAK between doublet 9312/0309 (Figures 1c and 5h), but PKiKP phases arrive at least 0.128 s and 0.054 s (residuals beyond the total travel time residual errors) later in the later events of doublets 9804/0912 and 9804/0403, respectively (Figures 1c and 5h). PKiKP-PKiKP differential travel times of these doublets further confirm that the travel time residuals are not caused by relative location and origin time of the doublets, as the PKiKP-PKiKP differential travel time would not be affected by the uncertainties of the origin times of the doublet and is affected little by uncertainties of relative location of the doublet. PKiKP-PKiKP differential travel times observed at AAK are 0.16 s, 0.08 s, and 0.08 s smaller in the later events of doublets 9804/0912, 9804/0403, and 0403/0912 (Figures 1c, 5d, and 5h, and Table 2). PKiKP/PKiKP amplitude ratio also exhibits change at AAK between the doublets 9804/0912, 9804/0403, and 0403/0912 (Figure 6d), with the most notable change of about a factor 2 for doublet 9804/0912. The temporal changes of the PKiKP travel time at ARU exhibit an opposite pattern from the early doublets 9312/0309, 9804/0912, and 0309/1003 to the later doublet 9807/1306. PKiKP phases arrive at similar time between doublets 9312/0309, 9804/0912, and 0309/1003, but at least 0.036 s later in the later event of doublet 9807/1306 (Figures 1b and 5g, and Table 2).

Because of the quality of the data, some of the doublet waveforms are compared in slightly different frequency bands from the filtering (the WWSSN-SP) we apply to the seismic data during doublet relocations. These seismic data include waveforms at ARU for doublet 9807/1306 (Figure 1a) and ALE for doublet 9911/0701 (Figure 6a) which are further filtered from 0.5 to 1.0 Hz, and waveforms at ARU for doublet 9804/0912 (Figure 1a) which are not filtered with the WWSSN-SP instrument response, but from 0.8 to 2.0 Hz. We show in section 3.2.5 that the error of studying the temporal change of the seismic data in these slightly different frequency bands is at most 0.01 s and would not affect the analysis results.

3.1.3. Temporal Changes of the PKiKP/PKiKP Coda Waves Sampling Africa

Some PKiKP/PKiKP coda waves sampling beneath Africa also exhibit temporal change, with the most prominent ones associated with those observations with prominent temporal changes of the main PKiKP or PKiKP waves. Note that the coda waves are clearly in misalignment in the observations at stations OBN, ARU, and AAK for doublet 9312/0309, at AAK for doublet 9804/0912, and at ARU for doublet 9807/1306 (Figure 6). Those coda wave temporal changes exhibit similar magnitude as those of the main waves. In contrast, there is less evident temporal change of PKiKP/PKiKP coda waves for those observations with no obvious temporal changes of the main PKiKP or PKiKP waves (Figure 6).

3.1.4. Temporal Changes of the PKiKP and PKiKP Waves Sampling Other Regions

No discernible temporal changes of PKiKP or PKiKP are observed for the seismic observations sampling other regions of the ICB for all the doublets occurring from 1993 to 2013 (Figure 7 and another example in Figure S9). Superimposed PKiKP-PKiKP waveforms of these doublets recorded at other stations show excellent agreements in both absolute arrival time and differential travel time of the two phases. There is no evident temporal change of PKiKP/PKiKP coda waves as well (Figures 7 and S9).

3.2. Exclusion of Possible Factors Other Than Temporal Change to Explain the PKiKP and PKiKP Changes Between the Doublets

We examine other possible factors that may explain the doublet difference of the PKiKP and PKiKP data sampling the inner core beneath Africa, without attributing it to temporal change of these IC phases. We show that the doublet difference of the PKiKP and PKiKP data sampling the inner core beneath Africa cannot be explained by the relative location or origin time of the doublets. Neither can it be explained by the effect of seismic noise, potential difference in source time function between the doublets, different frequency filtering, any temporal change near the source regions of the doublets, and seismic heterogeneities in the mantle.

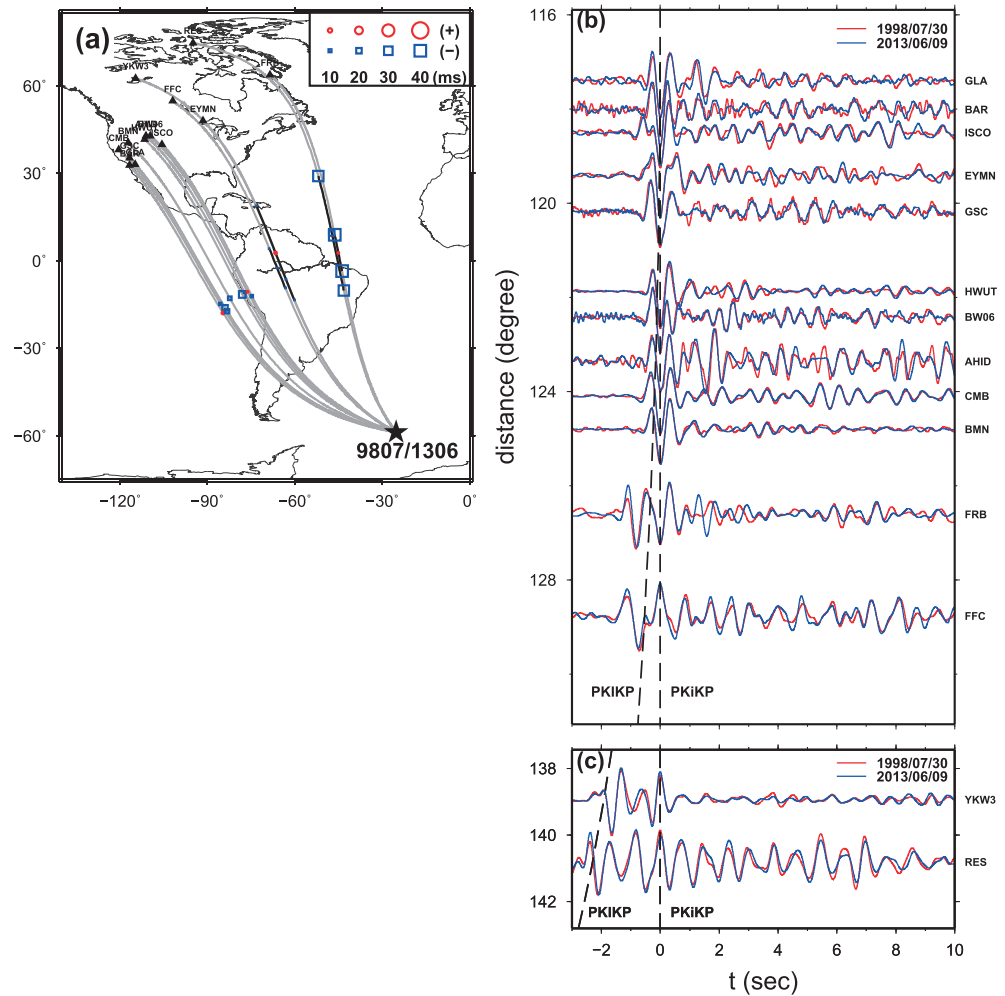


Figure 7. Temporal changes of PKiKP and PKIKP travel times between the doublets sampling other regions. (a) Travel time residuals of PKiKP and PKIKP phases between doublet 9807/1306, plotted at the reflected points of the inner core (for PKiKP residuals) or PKIKP entry and exit points at the ICB (for PKIKP residuals), along with the great circle paths (gray lines) from the doublet (star) to stations (triangles) and PKIKP raypaths in the inner core (black lines). Meaning of the symbols is the same as in Figure 5. (b) Superimposed PKiKP-PKIKP waveforms of doublet 9807/1306, aligned in the same way as in Figures 1b and 1c. The dashed lines are predicted arrivals of PKIKP and PKiKP phases based on IASP91 model [Kennett and Engdahl, 1991]. For display purposes, some traces are plotted at distances slightly away from their true epicentral distances.

3.2.1. Unreasonable Relative Location and Origin Time Difference Between the Doublet to Explain the PKIKP Arrival Times at AAK for Doublet 9804/0912

We discuss whether the PKIKP travel time difference observed at AAK between doublet 9804/0912 can be explained by a difference in event location or origin time between the doublet. A difference in event depth between the doublet cannot explain the data, because placing the later event shallower to reduce the negative 0.171 s residual (Table 2) of PKIKP phase at AAK would generate a similar amount of positive travel time residuals of PKiKP and PKIKP at other stations. We calculate the RMS travel time residuals and travel time residuals of the non-IC phases at each station for all possible relative event epicentral locations of the later event for doublet 9804/0912, by forcing the PKIKP arrival times between the doublet to fit within 0.033 s, the maximal relocation error at station TAU in Figure S1b. For each assumed event location of the later event, a relative origin time of the later event is found so that the PKIKP travel time residual at AAK is within 0.033 s. All relative event positions result in unacceptable RMS travel time residuals (Figure 8) and travel time residuals at many stations between the doublet (Figure 9). The above analysis indicates that the arrival time difference of the PKIKP phases recorded at AAK of the doublet cannot be explained by a difference in event location or origin time between the doublet.

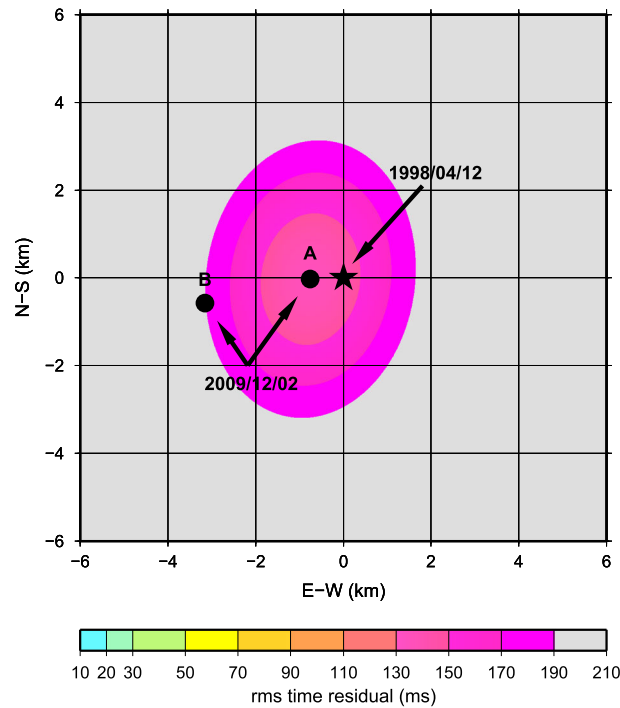


Figure 8. RMS travel time residuals of the non-IC phases as a function of relative location of event 2009/12/02 by forcing the travel time residual of the PKiKP phase observed at AAK between doublet 9804/0912 to be within 0.033 s. Two relative locations are labeled with one that generates the minimal RMS travel time residual among those that generate zero travel time residual of the PKiKP phase at AAK (dot labeled as A) and the other that produces a minimal RMS travel time residual among those that generate a zero mean of the travel time residuals of the non-IC phases between the doublet (dot labeled as B). The travel time residuals in individual stations between the doublet in these two cases are shown in Figures 9a and 9b, respectively.

3.2.2. Unreasonable Relative Location and Origin Time Difference Between the Doublet to Explain the Change of Differential PKiKP-PKiKP Travel Time Between the Doublet

The observed smaller differential PKiKP-PKiKP travel time of 0.16 s at station AAK in the later event of doublet 9804/0912 further confirms that the PKiKP travel time residual is not caused by relative event location or origin time of the doublet. The PKiKP-PKiKP differential travel time is insensitive to the uncertainties of the relative location between the two events. To generate a difference of 0.16 s in PKiKP-PKiKP differential travel time, a difference of 166 km (based on PREM) [Dziewonski and Anderson, 1981] or 127 km (based on IASP91) [Kennett and Engdahl, 1991] in epicentral distance is needed between the doublet and a difference in PKiKP absolute travel time of 3.01 s (based on PREM) or 2.31 s (based on IASP91) would result for that difference in epicentral distance. The PKiKP-PKiKP is even less sensitive to the event depth. A change of event depth from 100 km to 0 km would only yield a difference of 0.012 s (based on PREM) or 0.015 s (based on IASP91) in PKiKP-PKiKP differential travel time. All these scenarios can be excluded based on the measured arrival time differences of the doublet and the relocation analysis (Figure S1).

3.2.3. Little Effect of Noise on PKiKP and PKiKP Arrival Times and Waveforms

To test the effect of noise on PKiKP and PKiKP phases, we calculate synthetics by the generalized ray theory [Helmberger, 1983] and superimpose them with realistic noise that comes from different time windows before the PKiKP arrival in the data. Noise and synthetics are scaled according to the noise and signal ratio in the observations. We then check the waveforms and travel time differences between the synthetics with their respective noise between the doublets. We apply such procedure on the inner core phases that exhibit the most prominent temporal changes in the study, including the observed PKiKP and PKiKP phases recorded at station ARU for doublet 9807/1306 and at station AAK for doublet 9804/0912. There are no noticeable changes between the waveforms with their respective noise (Figure 10). The above analysis indicates that the observed temporal changes of PKiKP and PKiKP phases recorded at station ARU for doublet 9807/1306 and at station AAK for doublet 9804/0912 are not caused by noise.

3.2.4. Little Effect of Potential Difference of Source Time Function Between the Doublets on PKiKP and PKiKP Arrival Times and Waveforms

While most of the doublets have similar magnitudes, some do exhibit difference (Table 1). As a result, the source time function may be different between the doublets. We show that source time functions of the doublets are similar in the frequency bands of the study, and if any difference exists between them, it would not affect the analysis results in the text. We first note that in the frequency bands of the study, the observed waveforms of the non-IC phases (Figures 3 and S1–S7) and the IC phases (Figures 7 and S9) sampling the regions other than Africa are very similar between the doublets, as indicated by the comparisons of the waveforms and high cross-correlation coefficients between the doublet observations. The similarity of these observations indicates that the source time functions of the doublets are similar in the frequency bands of

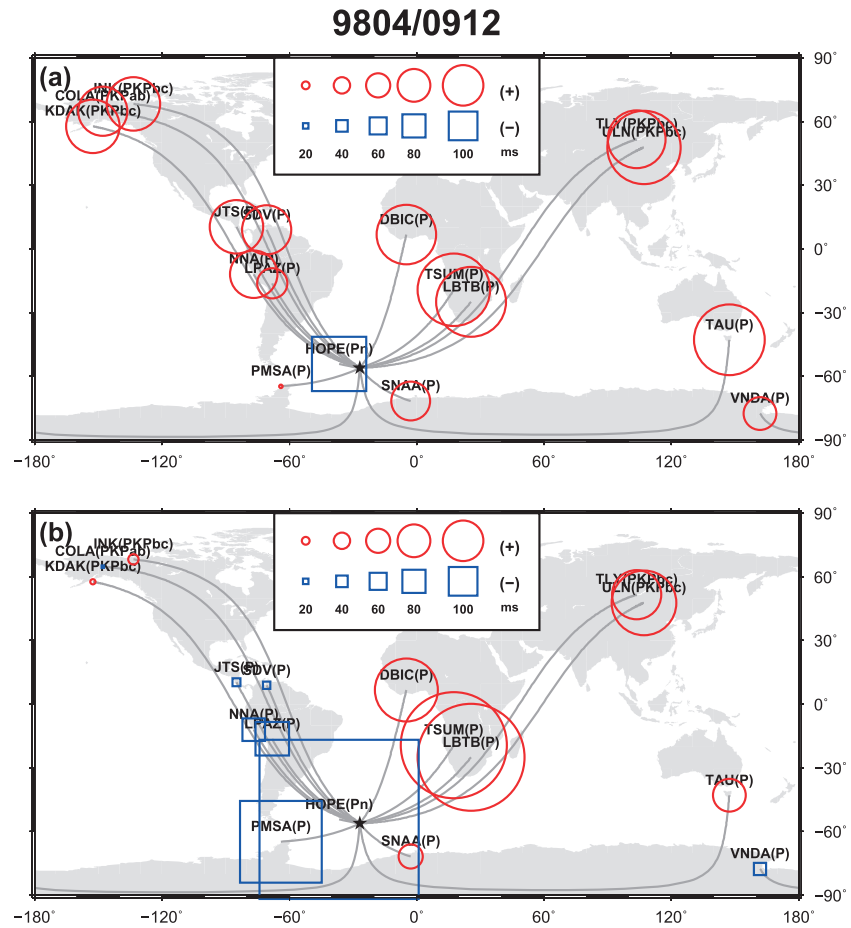


Figure 9. (a) Travel time residuals of the non-IC phases between doublet 9804/0912 for two example locations shown in Figure 8. Figures 9a and 9b are for the locations labeled as A and B in Figure 8, respectively. Meaning of the symbols is the same as in Figure 5.

the study. We perform further quantitative analyses to test the effect of potential change of source time function on PKiKP and PKiKP arrival times and waveforms, using two doublets 9804/0912 and 9807/1306 as examples. We convolve the observed waveforms of the earlier event of these doublets with Gaussian-shaped wavelets with various characteristic widths (Figure 11). Gaussian wavelets are defined as follows: $\frac{1}{A\sigma} * \left(e^{-2\left(\frac{t-t_s}{\sigma}\right)^2} - e^{-2\left(\frac{t_s}{\sigma}\right)^2} \right)$, with the characteristic width defined as $4 * \sqrt{2 \ln 2} * \sigma$ (A is a constant of 1.2533 and t_s is the center time of Gaussian wavelet). Convolution with a Gaussian wavelet is to simulate a scenario that the doublet may have different characteristic widths of source time functions. For doublet 9804/0912, a characteristic width larger than 0.7 s would distort the non-IC phase waveforms of the earlier event to be visibly different from the data comparison between the doublet (cf. the top trace with the middle of the bottom three traces in data examples in Figure 11a). With this characteristic width, the IC phase waveforms also exhibit some differences, but no visual offsets of the seismic phases are observed (the middle of the bottom three traces in data examples in Figure 11b). The difference of the IC phases in the doublet data is far more prominent, and visual offsets could be clearly observed (cf. the top trace with the middle of the bottom three traces in data examples in Figure 11b). For doublet 9807/1306, a characteristic width larger than 1.2 s would distort the non-IC phase waveforms of the earlier event to be visibly different from the data comparison between the doublet (cf. the top trace with the middle of the bottom three traces in data examples in Figure 11c). With this characteristic width, the IC phase waveforms also exhibit some differences, but no visual offsets of the seismic phases are observed, in contrast with the data comparisons where visual offsets could be clearly observed (cf. the top trace with the middle of the bottom three traces in data examples in Figure 11d). Thus, we

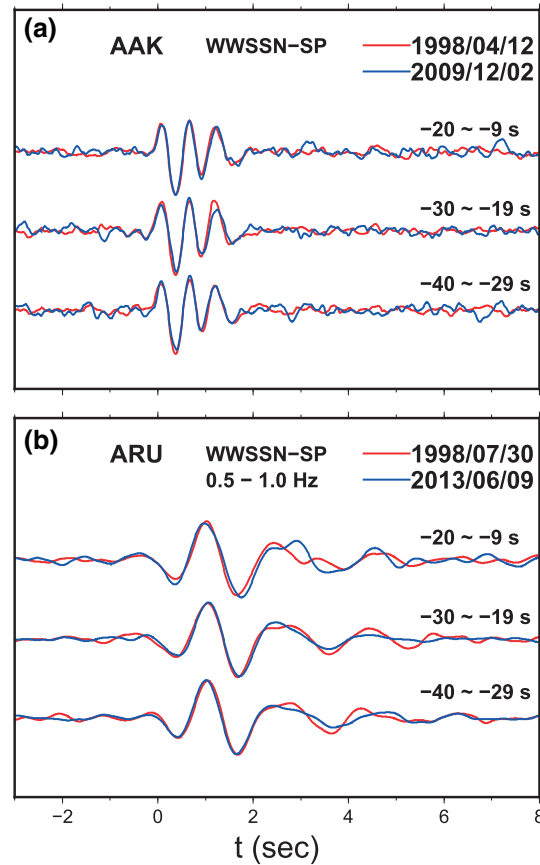


Figure 10. Examples of comparisons between PKiKP-PKiKP synthetics superimposed with noise recorded in various time windows of the observations from the earlier event (red traces) and later event (blue traces) of the doublets. The noise comes from various time windows (labeled in the top of each trace) before the PKiKP arrival in the data. (a) For doublet 9804/0912 and station AAK, the synthetics are filtered with the WWSSN-SP instrument response. (b) For doublet 9807/1306 and station ARU, the synthetics are first filtered with the WWSSN-SP instrument response and then from 0.5 to 1.0 Hz. All the filtering used in the synthetics is the same as that applied in the data. Synthetics are calculated by the generalized ray theory [Helmberger, 1983] and aligned along the predicted PKiKP arrival times based on PREM [Dziewonski and Anderson, 1981].

using the WWSSN-SP filtering are smaller than 0.2 km in both lateral location and event depth. The predicted arrival differences between the two relocation results are 0.01 s for the PKiKP and PKiKP phases at ARU for doublet 9807/1306 and 0.002 s for the PKiKP and PKiKP phases at ARU for doublet 9804/0912. For doublet 9911/0701, the new relocated depth has a slight trade-off with the relative origin time in comparison with the relocation results using the WWSSN-SP filtering, but they are still within 1.1 km. The difference of lateral location between the two relocations is only 0.1 km. The predicted arrival differences between the two relocation results are 0.004 s for the PKiKP and PKiKP phases at ALE. We thus conclude that the slightly different frequency filtering in some of the IC phases does not affect the inference of the temporal change of the IC phases.

3.2.6. Little Effect of Potential Temporal Change of Seismic Properties Near the Hypocenters or in the Mantle on the PKiKP-PKiKP Differential Travel Time

The temporal changes of PKiKP and PKiKP travel times at stations ARU and AAK between the doublets are unlikely caused by temporal changes of seismic properties near the hypocenters or in the mantle.

conclude that the observed differences of the IC phases are not caused by difference of source time function between the doublets.

3.2.5. Little Effect of Different Frequency Filtering on PKiKP and PKiKP Arrival Time Analysis

We relocate the doublets using seismic data filtered with the WWSSN-SP instrument response and then study the temporal change of the waveforms with the same filtering for most of the data, including those of prominent temporal changes, such as those at OBN, ARU, and AAK for doublet 9312/0309 and at AAK for doublets 9804/0912, 9804/0403, and 0403/0912 (Figures 1b and 1c). However, some of the doublet waveforms are compared in slightly different frequency bands because of the quality of the data. These seismic data include waveforms at ARU for doublet 9807/1306 (Figure 1a) and ALE for doublet 9911/0701 (Figure 6a) which are further filtered from 0.5 to 1.0 Hz, and waveforms at ARU for doublet 9804/0912 (Figure 1a) which are not filtered with the WWSSN-SP instrument response, but from 0.8 to 2.0 Hz. For these observations, it is necessary to estimate the errors of using the relocation results of the doublet based on the seismic data with a filtering scheme to study the difference of the seismic data in another frequency band. For those doublets involved, we also determine their relative location and origin time based on the seismic data filtered with the same filtering procedures used in examining the temporal change of the IC phases. In another word, we determine the relative location and origin time of doublets 9807/1306 and 9911/0701 using the frequency filtering applied to the seismic data at ARU and ALE, and those of doublet 9804/0912 based on the frequency filtering applied to the seismic data at ARU. For doublets 9807/1306 and 9804/0912, the differences between the relocation results using the new filtering and those

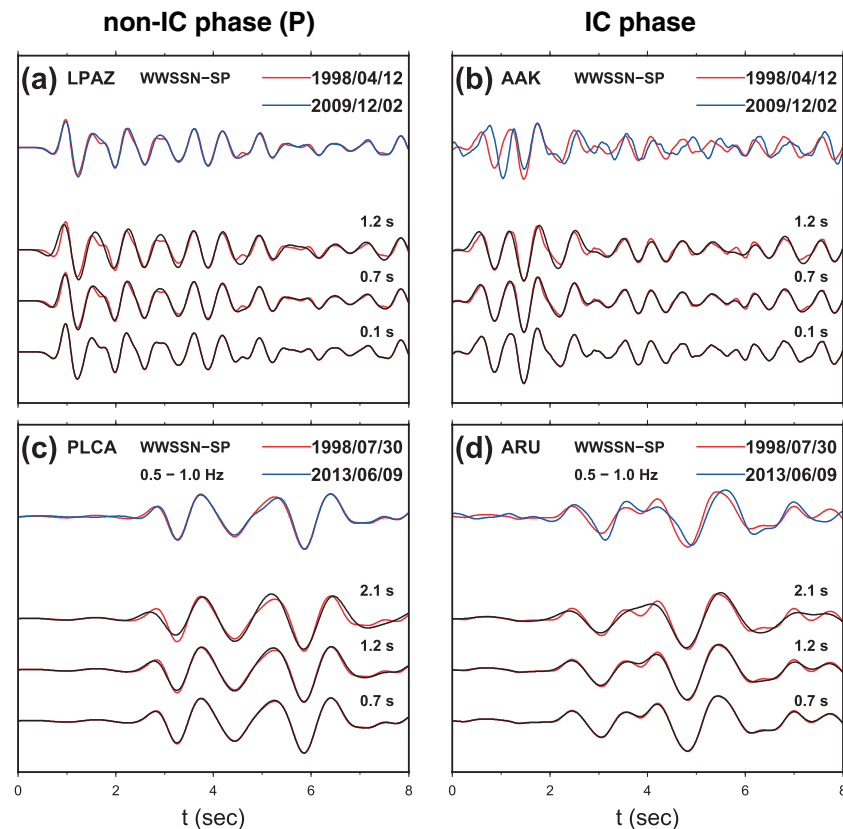


Figure 11. Examples of testing the effect of potential difference of source time function between the doublets on PKiKP and PKIKP arrival times and waveforms: (a and b) For doublet 9804/0912 and stations (a) LPAZ and (b) AAK, the waveforms are filtered with the WWSSN-SP instrument response; (c and d) for doublet 9807/1306 and stations (c) PLCA and (d) ARU, the waveforms are first filtered with the WWSSN-SP instrument response and then from 0.5 to 1.0 Hz. Top waveform pairs are the observed waveforms for the earlier (red trace) and later (blue traces) events in the doublets. The bottom waveform pairs are the waveforms of the earlier event (red traces) and their convolution with Gaussian wavelets with various widths (black traces), with the Gaussian widths labeled on the top of each trace. In the data comparisons (top traces in each panel), waveforms for the later event are aligned according to the travel times predicted based on the best fitting relative location and origin time of the doublets, while the bottom three traces in each panel are aligned on the handpicked arrival times.

Temporal change of seismic properties near the hypocenters would generate little change of PKiKP-PKIKP differential travel time between the doublets, as these phases have almost identical take-off angles (the difference is 0.43° for an example of AAK observations for doublet 9804/0912 based on PREM) from the earthquakes (Figure 1a). The temporal change of the seismic properties elsewhere in the mantle in such a short time scale is unlikely. But even if it exists, the PKiKP-PKIKP differential travel times are not sensitive to the seismic structures in the mantle as they have almost identical raypaths there (Figure 1a) [Niu and Wen, 2001; Wen and Niu, 2002].

3.2.7. Little Effect of Mantle Heterogeneities on PKiKP and PKIKP Travel Time Difference Between the Doublets

The observed temporal changes of PKiKP and PKIKP travel times cannot be caused by seismic heterogeneities in the mantle. The horizontal separations of the raypaths of a seismic phase (either PKiKP or PKIKP) between the doublets are all smaller than 0.5 km (0.5 km, 0.1 km, and 0.2 km for doublets 9312/0309, 9804/0912, and 9807/1306, respectively) at every depth in the mantle. These separations are at least 60 times smaller than the widths of the Fresnel zones of the seismic phase, for the domain frequency of the seismic signals. Therefore, if a mantle seismic scatterer distorts the raypath of a particular phase, it would do so in the same way between the doublet. Based on the distance separations of the doublets, the raypath distortion of any seismic heterogeneity in the mantle would not generate the magnitude of travel time difference that is comparable with those observed between the doublets. For example, if we assume that the PKIKP raypaths are scattered

and deviated from the theoretical great circle paths, the maximum predicted travel time difference at station AAK between doublet 9804/0912 is only $-0.03 \sim +0.03$ s based on the separation of the doublet and for any seismic heterogeneities in the mantle, while the observed PKiKP travel time difference is up to -0.155 s (the observed arrival time difference adjusted by the best fitting relative origin time). Thus, we conclude that the observed differences of absolute travel time of the IC phases between the doublets are not caused by seismic heterogeneities in the mantle.

The observed PKiKP-PKiKP differential travel time residuals between the doublets cannot be caused by seismic heterogeneities in the mantle either. The horizontal separations between PKiKP and PKiKP raypaths of the same event are much smaller than Fresnel zones of seismic waves in the shallow mantle (e.g., the separations of the two seismic raypaths are 2.4 km for doublet 9312/0309 and 1.7 km for doublet 9804/0912 at a depth of 300 km, more than 20 times smaller than the widths of Fresnel zones of the seismic phases). Therefore, if a seismic scatterer at shallow depth distorts the raypaths of one seismic phase (either PKiKP or PKiKP), it would do so in the same way for the other seismic phase. In this case, PKiKP-PKiKP differential travel time residual between the doublet would be zero. The separations of the raypaths of PKiKP and PKiKP phases in the deep mantle are also within the Fresnel zones of the seismic waves (e.g., the separations of the two seismic raypaths are about 40 km for doublets 9312/0309 and 9804/0912 at the core-mantle boundary, at least three times smaller than the widths of Fresnel zones of the seismic phases), and it is reasonable to assume that a seismic scatterer in the deep mantle would distort both the PKiKP and PKiKP raypaths in the same way, and PKiKP-PKiKP differential travel time residual between the doublet is negligible. Even if we assume that seismic scatterers in the deep mantle could distort these two seismic phases independently, they would not generate a magnitude of PKiKP-PKiKP differential travel time that is comparable with those observed between the doublets. For example, if we assume that raypaths of PKiKP and PKiKP phases are scattered independently away from the theoretical great circle paths, the maximum predicted PKiKP-PKiKP differential travel time residual at station AAK between doublet 9804/0912 is $-0.02 \sim +0.02$ s based on the separation of the doublet and for any seismic heterogeneities 300 km deeper in the mantle that would not produce a PKiKP-PKiKP differential travel time beyond 1 s of PREM prediction (the maximal deviation of PKiKP-PKiKP differential travel time observed in the global data set) [Niu and Wen, 2001; Wen and Niu, 2002]. The observed difference of the PKiKP-PKiKP differential travel time between the doublet is, however, 0.16 s. Thus, we conclude that the observed differential travel times of the IC phases between the doublets are not caused by seismic heterogeneities in the mantle.

3.3. Temporal Change of the Earth's Inner Core Surface Beneath Africa

Temporal change of PKiKP travel time can only be explained by change of inner core radius at the PKiKP reflected point at the ICB [Wen, 2006]. Decreasing inner core radius would produce a later PKiKP arrival, because the PKiKP wave would be reflected at a larger depth. Increasing inner core radius would do the opposite. Temporal change of PKiKP travel time can also be explained by change of inner core radius at either the entry or exit point of the PKiKP waves at the ICB, or both. Decreasing inner core radius would produce a later PKiKP arrival, as the PKiKP wave would propagate a larger distance in the outer core that has a relatively small compressional wave velocity than the inner core and a smaller distance in the inner core (Figures 12a–12c). PKiKP and PKiKP waves could also respond separately to localized temporal change of the inner core surface, as the separation of the two phases at the ICB (e.g., 190 km for AAK observations of doublet 9804/0912) is larger than the width of the Fresnel zone of seismic phases (e.g., about 170 km for the PKiKP phase), for the domain frequency of the seismic signals (Figure S10). For similar reasons, temporal change of PKiKP/PKiKP amplitude ratio and PKiKP/PKiKP coda waves could also be explained by temporal change of the inner core surface [Wen, 2006], as PKiKP and PKiKP amplitudes, as well as their coda, could be affected considerably by ICB topography [Cao *et al.*, 2007; Dai *et al.*, 2012; Wen, 2006].

The history and geographical distribution of the temporal change of the inner core surface beneath Africa is inferred based on the observed temporal changes of PKiKP and PKiKP travel times of the observations at OBN, ARU, and AAK (Figure 4b and Table 2) (see section 4 for discussion on the alternatives of explanations). As the Fresnel zones of seismic phases for each group of observations in Figure 4b significantly overlay at the ICB (Figure S10), we regard that the observations in each individual group reflect the temporal changes of the

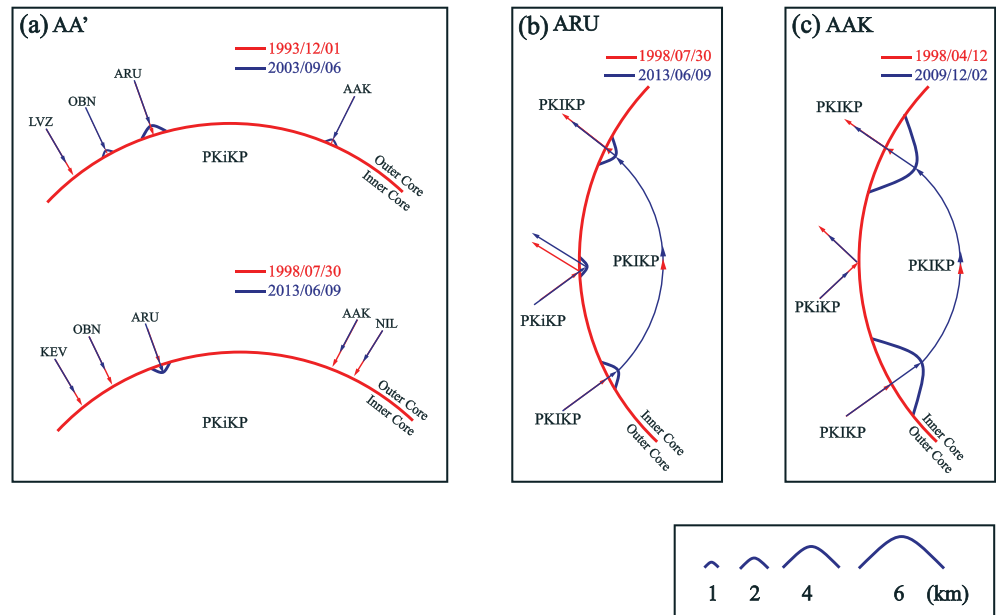


Figure 12. (a–c) Schematic illustration of temporal change of the inner core surface along three cross sections beneath Africa (green and red lines in Figure 4a), with the boundary at an earlier time in red and a later time in blue. PKiKP reflection points and PKiKP entry and exit points at the ICB are illustrated by arrows, along with the portion of PKiKP path in the inner core.

same sampling region at the ICB and discuss them collectively in the history of available doublets. The travel time change related to temporal change of the inner core surface is calculated based on the method of *Buland and Chapman* [1983]. All the reported values of the ICB change are estimated based on the observed travel time residuals between the doublets beyond the total possible travel time residual error (relocation error plus 0.01 s of travel time picking error) of each doublet.

In the earlier period (before 2003, between the occurrences of doublet 9312/0309), inner core surface is enlarged by 0.53–1.78 km beneath the western coast of Gabon, Republic of Congo, and southwest Tanzania (at the PKiKP reflection points of the observations at OBN, ARU, and AAK) (regions b, c, and d, Figures 4a, 4b, and 12a), but exhibits little change beneath Zimbabwe or/and Kenya (near the PKiKP entry or/and exit point for AAK observations) (region h, Figures 4a and 4b).

In the later period (after 1998), the inner core surface keeps unchanged between 1998 and 2013 beneath the western coast of Gabon and southwest Tanzania (at the PKiKP reflected points of the OBN and AAK observations) (regions b and d, Figures 4a, 4b, and 12a); the inner core radius decreases by at least 1.16 km between 1998 and 2013 beneath Republic of Congo (at the PKiKP reflection point of ARU observations) (region c, Figures 4a, 4b, 12a and 12b), but with no detectable change between the occurrences of doublets 9804/0912 [with detection limit of 1.08 km (Table 3)] and 0309/1003 [with detection limit of 0.59 km (Table 3)]. Unlike the earlier period between doublet 9312/0309, in which it experiences little change, the inner core radius experiences a significant decrease by at least 5.59 km between the occurrences of doublet 9804/0912 beneath Zimbabwe or Kenya (near the PKiKP entry or exit point for AAK observations) (region h, Figures 4a, 4b, and 12c). Inner core radius decreases by 1.73 km beneath west Angola or north Central African Republic (near the PKiKP entry or exit point of ARU observations) (region g, Figures 4a, 4b, and 12b) between the occurrences of doublet 9807/1306, while no changes of inner core radius are observed beyond uncertainties between doublets 9312/0309, 9804/0912, and 0309/1003 (although the inner core radius may be enlarged by 1.93 km between the occurrences of doublet 9312/0309, decreased by 1.35 km between doublet 9804/0912, and enlarged by 1.12 km between doublet 0309/1003) (Table 3), but we should emphasize that these numbers are within the detection limits of these doublets. These results indicate that the temporal change of the inner core surface beneath Africa in the last 20 years is episodic, rapidly migrating and alternately constructive and destructive.

Table 3. Estimates of Temporal Changes of the Radius of the Inner Core Surface^a

Station	Doublet ID	PKiKP		PKIKP	
		ΔR_{ICB} (km)	DL (km)	ΔR_{ICB} (km)	DL (km)
KEV	9807/1306	0.79	0.94	0.05	1.74
LVZ	9312/0309	-0.66	1.08	-0.40	2.01
DAG	0308/0905	-1.27	1.00	0.44	1.84
ALE	0802/1102	0.10	1.51	1.45	2.50
	9911/0701	-0.57	1.06	-1.31	1.76
	9312/0309	0.99	1.76	2.71	2.78
KIEV	0308/0905	-0.05	0.52	-	-
OBN	9807/1306	0.39	0.64	-	-
	9312/0309	1.27	0.74	-	-
ARU	9807/1306	-2.06	0.90	-3.37	1.64
	0309/1003	0.47	0.59	1.12	1.12
	9804/0912	-1.03	1.08	-1.35	2.01
	9312/0309	2.84	1.06	1.93	1.93
AAK	9807/1306	0.16	0.79	-	-
	0403/0912	0.05	1.10	-3.39	2.10
	9804/0403	-0.12	0.72	-3.68	1.40
	9804/0912	-0.25	1.00	-7.46	1.87
	9312/0309	1.54	0.95	-1.79	1.79
XAN	9807/1306	-0.30	1.45	0.95	2.48
	9312/0309	-1.13	1.85	-0.14	2.89
CHTO	9807/1306	-0.15	0.63	-	-
	9312/0309	0.00	0.77	-	-
LSA	9807/1306	-0.70	0.75	0.71	1.42
NIL	9807/1306	0.00	0.60	-	-

^a ΔR_{ICB} : temporal change of the radius of the inner core surface corresponding to PKiKP or PKIKP travel time residual (ΔT_{PKiKP}^{res} or ΔT_{PKIKP}^{res}) between the doublet (Table 2). DL: detection limit of temporal change of the radius of the inner core surface corresponding to travel time residual error, dt_{err} .

4. ICB Change as the Favorable Explanation for the Observed Temporal Change of the PKiKP and PKIKP Waves

Wen [2006] suggested that the enlargement of inner core radius beneath mid-Africa (observed between doublet 9312/0309) could be explained by two mechanisms: (1) a rapid localized enlargement of inner core radius between the occurrences of doublet 9312/0309 or (2) a differential inner core rotation assuming that irregularities are present at the ICB and fixed to the inner core. However, the observation that the temporal change of PKiKP travel time changes characteristics from the earlier doublet (9312/0309) to later period is too much a coincidence for the differential inner core rotation interpretation. The inner core would have rotated into the PKiKP sampling points of AAK, ARU, and OBN observations from topographic low regions to topographic high regions at the same time during the early period (9313/0309) and rotated a flat topography into all these PKiKP sampling points during the later period also at a same onset time (after 1998), despite of the random distribution of the PKiKP sampling points in the inner core surface.

The inference of an inner core differential rotation was based on the seismic evidence that the PKIKP waves (or their coda) changed over time [Creager, 1997; Leyton and Koper, 2007; Song and Richards, 1996; Vidale et al., 2000; Zhang et al., 2005]. Such changes can also be explained by temporal change of inner core surface. On one hand, the temporal change of the PKiKP phases can only be explained by temporal change of inner core surface and the magnitude of the inner core surface change inferred from the PKiKP temporal change also sufficiently explains the PKIKP temporal changes. On the other hand, the inference of an inner core differential rotation has evolved to have to appeal to an axisymmetric anisotropic structure, existence of irregularities at the inner core surface and being rotated with the inner core (for explaining PKiKP temporal changes), and now to be too much a coincidence in explaining longer time period of temporal change of inner core surface reported here. The proposed differential inner core rotation is also dynamically inconsistent with the observed hemispherical variation of seismic structure in the top of the inner core [Cao and Romanowicz, 2004; Niu and Wen, 2001; Tanaka and Hamaguchi, 1997; Wen and Niu, 2002]. From the above considerations, it is our opinion that the temporal change of inner core surface provides the

simpler explanation for all the observations of temporal changes of the core phases and removes the inconsistency between the proposed differential inner rotation and the observed hemispheric variation of seismic structure at the top of the inner core.

5. Possible Mechanisms and Implications

The change of inner core surface may be caused by two mechanisms: (1) a regional perturbation of temperature and/or composition near the ICB and that the time scale for the ICB surface to adjust to the regional change of temperature and composition is similar to or shorter than that of the temperature/composition change, and (2) deformation of inner core surface by small-scale force near the ICB and that the time scale for the deformed boundary to readjust to the phase equilibrium is longer than the time scale of deformation. In the first scenario, the position of the ICB could be quickly adjusted to be a solid-liquid phase boundary in equilibrium with the local temperature and composition, and it changes as the local temperature and/or composition change. The increase of inner core radius would mean solidification of additional inner core material from the outer core, while the decrease of inner core radius would mean remelting of some inner core material. In the second scenario, the inner core surface is deformed out of its equilibrium phase boundary by small-scale force near the ICB and some degree of the deformation is maintained due to a longer time scale for the deformed boundary to be completely re-equilibrated with the thermo-compositional condition at the ICB. The increase of inner core surface would place some inner core materials out of the equilibrium boundary and into the liquid regime, resulting in remelting of the inner core materials, while the decrease of the inner core surface would place some outer core material into the solid regime, resulting in solidification of the outer core materials.

The temporal change of inner core surface is intimately related to the driving forces of the outer core convection and geodynamo. The solidification of additional inner core material from the outer core would release latent heat and light elements, producing one type of the thermo-compositional driving force, while the remelting of some inner core material would absorb latent heat and light elements, generating an opposite type of the thermo-compositional driving force. Our seismic results indicate that the energy release associated with the inner core solidification/melting is not geographically uniform, with the intensive energy release occurring in a very short time scale (years or smaller) and localized in some geographic regions. In the localized region of intense energy release, the driving forces are episodic, rapidly migrating and alternately changing signs.

Song and Dai [2008] suggested that it is difficult to appeal for the mechanism of localized growth to explain the temporal change of PKiKP phase, as it would require a short time scale of inner core solidification/melting. They suggested another mechanism that slurry patches might exist in some regions of the ICB, containing a mixture of molten materials and solidification crystals. These slurry patches may be moved along the inner core surface driven by outer core convection, causing the observed temporal change of PKiKP waves. They suggested this model could provide a good explanation, as it does not require solidification or melting in a short time scale.

We should point out that the time scale of localized solidification or melting in the inner core boundary is unknown, and any argument appealing a presumed long time scale against a physical mechanism does not have the supporting scientific evidence. What is known is that the average growth rate of the inner core must be very slow based on the radius and age of the Earth's inner core. However, it is now clear that the inner core surface is irregular and such irregularities are localized, and inner core growth could be constructive and destructive in some localized regions. It is entirely possible that the time scale of localized solidification and melting is short while maintaining the slow average growth rate of the inner core.

A slurry patch, if it exists, would be intimately associated with the local thermo-compositional state of the bottom of the outer core. A slurry patch would not maintain its physical state in the outer core when it is moved out of its location of generation, as the thermo-compositional condition in the new hosting bottom of the outer core would re-equilibrate the slurry patch to be the outer core material. That is, thermo-compositionally, a slurry patch cannot survive as independent, freely moving "sediment" in the bottom of the outer core.

6. Conclusions

We study two decades of temporal change behavior of the Earth's inner core surface by analyzing the temporal changes of PKiKP and PKiKP travel times of earthquake waveform doublets occurring in SSI between 1993 and

2013. These doublets are within 1 km of separation of depth and horizontal distance. The temporal changes of the PKiKP and PKiKP waves are only observed in the doublet data recorded at three seismic stations, OBN, AAK, and ARU, with sampling points in the inner core surface beneath Africa. PKiKP phases observed at the three stations arrive at least 0.026 to 0.07 s earlier in the 2003 event as compared to the 1993 event in doublet 9312/0309, but PKiKP phases observed at OBN and AAK arrive almost at the same time for the doublets in the later periods and arrive at least 0.044 s later at ARU in the later event for doublet 9807/1306. No discernible PKiKP travel time difference is observed at AAK between doublet 9312/0309, but PKiKP phase arrives at least 0.128 s later in the later event for doublet 9804/0912. PKiKP phases recorded at ARU arrive at a similar time in the earlier periods but at least 0.036 s later in the later event of doublet 9807/1306.

The history and geographical distribution of the temporal change of the inner core surface beneath Africa is then inferred based on the observed temporal changes of PKiKP and PKiKP travel times. In the early period (before 2003), the inner core surface is enlarged by 0.53–1.78 km beneath the western coast of Gabon, Republic of Congo, and southwest Tanzania in the reflected points of the PKiKP observations at OBN, ARU, and AAK, while the regions beneath Zimbabwe or/and Kenya and beneath west Angola or/and north Central African Republic (in the PKiKP entry or/and exit point of AAK and ARU observations, respectively) experience little change. In the later period (after 1998), the ICB regions beneath the western coast of Gabon, Republic of Congo, and southwest Tanzania (at the PKiKP reflected points) either shrink or remain unchanged, and the temporal change migrates to the inner core surface beneath Zimbabwe or/and Kenya, and beneath west Angola or/and north Central African Republic (in the PKiKP entry or/and exit point), with decrease of inner core surface by up to 5.59 km between 1998 and 2009 beneath Zimbabwe or Kenya, and by 1.73 km beneath west Angola or north Central African Republic between 1998 and 2013. These seismic results indicate that the temporal change of the inner core surface occurs in localized regions and is episodic, rapidly migrating and alternately enlarged and shrunk in a time scale of years.

Acknowledgments

We thank Peter Shearer, Satoru Tanaka, and two anonymous reviewers for their comments and suggestions that have significantly improved the paper. The seismic data are downloaded from the Incorporated Research Institutions for Seismology (IRIS), and we gratefully acknowledge the IRIS for the high-quality data. This work is supported by the National Natural Science Foundation of China under grant NSFC41130311 and the Chinese Academy of Sciences and State Administration of Foreign Experts Affairs International Partnership Program for Creative Research Teams.

References

- Braginsky, S. I. (1963), Structure of the F layer and reasons for convection in the Earth's core, *Dokl. Akad. Nauk SSSR*, *149*, 1311–1314.
- Buffett, B. A. (2000), Dynamics of the Earth's core, in *Earth's Deep Interior: Mineral Physics and Tomography from the Atomic to the Global Scale*, *Geophys. Monogr. Ser.*, vol. 117, edited by S.-I. Karato et al., pp. 37–62, the AGU, Washington, D. C.
- Buland, R., and C. H. Chapman (1983), The computation of seismic travel times, *Bull. Seismol. Soc. Am.*, *73*(5), 1271–1302.
- Cao, A., and B. Romanowicz (2004), Hemispherical transition of seismic attenuation at the top of the earth's inner core, *Earth Planet. Sci. Lett.*, *228*(3–4), 243–253, doi:10.1016/j.epsl.2004.09.032.
- Cao, A., Y. Masson, and B. Romanowicz (2007), Short wavelength topography on the inner-core boundary, *Proc. Natl. Acad. Sci. U.S.A.*, *104*(1), 31–35.
- Creager, K. C. (1997), Inner core rotation rate from small-scale heterogeneity and time-varying travel times, *Science*, *278*(5341), 1284–1288, doi:10.1126/science.278.5341.1284.
- Dai, Z., W. Wang, and L. Wen (2012), Irregular topography at the Earth's inner core boundary, *Proc. Natl. Acad. Sci. U.S.A.*, *109*(20), 7654–7658.
- Davies, G. F. (1979), Timing of core formation and onset of the geomagnetic dynamo in convecting Earth models Paper 10/30, *XVII General Assembly, IUGG*, Canberra.
- Dziewonski, A. M., and D. L. Anderson (1981), Preliminary reference Earth model, *Phys. Earth Planet. Inter.*, *25*(4), 297–356, doi:10.1016/0031-9201(81)90046-7.
- Dziewonski, A. M., T. A. Chou, and J. H. Woodhouse (1981), Determination of earthquake source parameters from waveform data for studies of global and regional seismicity, *J. Geophys. Res.*, *86*(B4), 2825–2852, doi:10.1029/JB086iB04p02825.
- Ekström, G., M. Nettles, and A. M. Dziewoński (2012), The global CMT project 2004–2010: Centroid-moment tensors for 13,017 earthquakes, *Phys. Earth Planet. Inter.*, *200–201*, 1–9, doi:10.1016/j.pepi.2012.04.002.
- Fearn, D. R., D. E. Loper, and P. H. Roberts (1981), Structure of the Earth's inner core, *Nature*, *292*, 232–233.
- Gubbins, D. (1977), Energetics of the Earth's core, *J. Geophys.*, *43*, 453–464.
- Helmburger, D. (1983), Theory and application of synthetic seismograms, in *Earthquakes: Observation, Theory and Interpretation*, vol. 37, edited by H. Kanamori, pp. 173–222, Soc. Ital. di Fis., Bologna, Italy.
- Jacobs, J. A. (1953), The Earth's inner core, *Nature*, *172*(4372), 297–298.
- Kennett, B. N., and E. Engdahl (1991), Traveltimes for global earthquake location and phase identification, *Geophys. J. Int.*, *105*(2), 429–465.
- Leyton, F., and K. D. Koper (2007), Using PKiKP coda to determine inner core structure: 1. Synthesis of coda envelopes using single-scattering theories, *J. Geophys. Res.*, *112*, B05316, doi:10.1029/2006JB004369.
- Li, A., and P. G. Richards (2003), Using earthquake doublets to study inner core rotation and seismicity catalog precision, *Geochem. Geophys. Geosyst.*, *4*(9), 1072, doi:10.1029/2002GC000379.
- Long, H., and L. Wen (2012), Using repeated sources to quantitatively determine temporal change of medium properties: Theory and an example, *J. Geophys. Res.*, *117*, B09303, doi:10.1029/2012JB009302.
- Loper, D. E. (1978), The gravitationally powered dynamo, *Geophys. J. Int.*, *54*(2), 389–404.
- Loper, D. E., and P. H. Roberts (1981), A study of conditions at the inner core boundary of the Earth, *Phys. Earth Planet. Inter.*, *24*(4), 302–307.
- Niu, F., and L. Wen (2001), Hemispherical variations in seismic velocity at the top of the Earth's inner core, *Nature*, *410*(6832), 1081–1084.
- Poupinet, G., and A. Souriau (2001), Reply to Xiadong Song's comment on "The existence of an inner core super-rotation questioned by teleseismic doublets", *Phys. Earth Planet. Inter.*, *124*(3), 275–279.

- Poupinet, G., W. Ellsworth, and J. Frechet (1984), Monitoring velocity variations in the crust using earthquake doublets: An application to the Calaveras Fault, California, *J. Geophys. Res.*, *89*(B7), 5719–5731, doi:10.1029/JB089iB07p05719.
- Poupinet, G., A. Souriau, and O. Coutant (2000), The existence of an inner core super-rotation questioned by teleseismic doublets, *Phys. Earth Planet. Inter.*, *118*(1), 77–88.
- Song, X. (2001), Comment on “The existence of an inner core super-rotation questioned by teleseismic doublets” by Georges Poupinet, Annie Souriau, and Olivier Coutant, *Phys. Earth Planet. Inter.*, *124*(3), 269–273.
- Song, X., and W. Dai (2008), Topography of Earth’s inner core boundary from high-quality waveform doublets, *Geophys. J. Int.*, *175*(1), 386–399.
- Song, X., and P. G. Richards (1996), Seismological evidence for differential rotation of the Earth’s inner core, *Nature*, *382*(6588), 221–224.
- Stevenson, D. J. (1987), Limits on lateral density and velocity variations in the Earth’s outer core, *Geophys. J. R. Astron. Soc.*, *88*(1), 311–319, doi:10.1111/j.1365-246X.1987.tb01383.x.
- Stevenson, D. J., T. Spohn, and G. Schubert (1983), Magnetism and thermal evolution of the terrestrial planets, *Icarus*, *54*(3), 466–489.
- Tanaka, S., and H. Hamaguchi (1997), Degree one heterogeneity and hemispherical variation of anisotropy in the inner core from PKP (BC)–PKP(DF) times, *J. Geophys. Res.*, *102*(B2), 2925–2938, doi:10.1029/96JB03187.
- Tkalčić, H., M. Young, T. Bodin, S. Ngo, and M. Sambridge (2013), The shuffling rotation of the Earth’s inner core revealed by earthquake doublets, *Nat. Geosci.*, *6*(6), 497–502.
- Vidale, J. E., D. A. Dodge, and P. S. Earle (2000), Slow differential rotation of the Earth’s inner core indicated by temporal changes in scattering, *Nature*, *405*(6785), 445–448.
- Wen, L. (2006), Localized temporal change of the Earth’s inner core boundary, *Science*, *314*(5801), 967–970.
- Wen, L., and F. Niu (2002), Seismic velocity and attenuation structures in the top of the Earth’s inner core, *J. Geophys. Res.*, *107*(B11), 2273, doi:10.1029/2001JB000170.
- Wiggins, R. A. (1976), Interpolation of digitized curves, *Bull. Seismol. Soc. Am.*, *66*(6), 2077–2081.
- Yoshida, S., I. Sumita, and M. Kumazawa (1996), Growth model of the inner core coupled with the outer core dynamics and the resulting elastic anisotropy, *J. Geophys. Res.*, *101*(B12), 28,085–28,103, doi:10.1029/96JB02700.
- Zhang, J., X. Song, Y. Li, P. G. Richards, X. Sun, and F. Waldhauser (2005), Inner core differential motion confirmed by earthquake waveform doublets, *Science*, *309*(5739), 1357–1360.
- Zhang, J., P. G. Richards, and D. P. Schaff (2008), Wide-scale detection of earthquake waveform doublets and further evidence for inner core super-rotation, *Geophys. J. Int.*, *174*(3), 993–1006.